

# A novel method for preparing epoxy-containing microcapsules via UV irradiation-induced interfacial copolymerization in emulsions

Ding Shu Xiao<sup>a</sup>, Min Zhi Rong<sup>b,\*</sup>, Ming Qiu Zhang<sup>b</sup>

<sup>a</sup> Key Laboratory for Polymeric Composite and Functional Materials of Ministry of Education, OFCM Institute, School of Chemistry and Chemical Engineering, Zhongshan University, Guangzhou 510275, PR China

<sup>b</sup> Materials Science Institute, Zhongshan University, Guangzhou 510275, PR China

Received 25 February 2007; received in revised form 7 June 2007; accepted 10 June 2007

Available online 15 June 2007

## Abstract

A novel method for producing epoxy resin-containing microcapsules via UV-initiated radical copolymerization in an epoxy emulsion was developed. Epoxydiacrylates and a polymerizable emulsifier were employed as the wall-formers, which tended to accumulate at the exterior layer of epoxy colloids during the emulsification process. Upon exposure to UV light, the shell phase consisting of the wall-formers was rapidly cured into solid to generate microcapsules with epoxy as the core substance. In this paper, the characteristics of the resultant microcapsules, including size and size distribution, chemical features, surface morphology, thermal stability, core content, and reactivity with curing agent, were studied. Also, the factors influencing the preparation of microcapsules were analyzed. Moreover, the optimum synthetic conditions of UV irradiation to prepare the microcapsules were determined by orthographic factorial design. Compared to the conventional thermal initiation, the present UV-aided encapsulation saves time.

© 2007 Elsevier Ltd. All rights reserved.

**Keywords:** Microcapsules; Epoxy resin; UV irradiation

## 1. Introduction

Microcapsules and microcapsule technology have been widely employed in a series of fields including recording media [1], medical supplies [2], foods [3], industrial materials [4], etc. Recently, microcapsules containing liquid healing agent were found to be applicable for making self-healing polymeric composites [5]. The working principle is based on the fact that microencapsulated healing agent is pre-embedded in the target polymer. Having been broken, these microcapsules release the repair substance into the cracked planes and re-bond them. Poly(urea-formaldehyde) (PUF) microcapsules are the most used systems for this purpose. Several groups sealed dicyclopentadiene (DCPD) [5] and epoxy [6–8] in PUF microcapsules. However, the synthesis of PUF microcapsules is somewhat complicated and time-consuming

for mass production and large-scale application [9,10]. Development of new approaches for preparing a microencapsulated healing agent is necessary.

Interfacial phenomena related to physico-chemical processes (like adsorption/desorption, deposition and mass transport) and chemical reactions (e.g., polycondensation, in situ polymerization and polyaddition) are the major procedures for carrying out microencapsulation [11]. The methods often used in practice include: spray drying, phase separation from a continuous phase, solvent extraction, layer-by-layer addition, solvent evaporation, and interfacial polymerization utilizing emulsions and microemulsions [12]. To the authors' knowledge, however, ultraviolet (UV) irradiation-induced radical polymerization has not yet been applied to the preparation of microcapsules. Quek et al. [13] established a crosslinking structure using UV light in the exterior wall made from polyelectrolyte copolymer to enhance mechanical strength and chemical stability of microcapsules. Similarly, Shen et al. [14] improved the stability of alginate hydrogel microcapsules by developing a photo-crosslinked interpenetrating polymer

\* Corresponding author.

E-mail address: [cesrmz@mail.sysu.edu.cn](mailto:cesrmz@mail.sysu.edu.cn) (M.Z. Rong).

network with photo-polymerized sodium acrylate and *N*-vinyl pyrrolidone. In these works photo-crosslinking was only used to strengthen capsules' wall.

Photopolymerization offers some distinct advantages like rapid reaction, lower energy consumption and less environmental pollution. Thereby, the authors of the present work propose herein a route to produce epoxy resin-containing microcapsules by means of UV-initiated radical copolymerization between epoxydiacrylates and a polymerizable emulsifier (sodium 3-methacryloyloxy-2-hydroxy propane sulphonate (trade name: HPMAS)).

Epoxydiacrylate was chosen as the wall-former because it is a derivative from epoxy (the core substance to be encapsulated), and is able to establish strong interaction with the emulsifier. Besides, it is photosensitive and often used in UV cured coatings [15]. Furthermore, the polymerizable emulsifier played a key role in this technique. It not only stabilized the emulsion but also took part in the formation of the shells. To favor accumulation of epoxydiacrylates around the epoxy colloids, an additional emulsifier, styrene–maleic anhydride (SMA) copolymer, was incorporated to increase the interfacial interaction between epoxydiacrylates and emulsifier.

The epoxy-containing microcapsules obtained via the above route were carefully characterized. The influence of the processing parameters was also discussed. In particular, the UV irradiation conditions were optimized employing orthogonal factorial design.

## 2. Experimental and methods

### 2.1. Materials

Two kinds of epoxy resins, the diglycidyl ether of bisphenol A (trade name: E-51) and the diglycidyl ether of tetrahydrogen phthalic acid (trade name: E-711), to be used as the core materials of the microcapsules, were provided by Dongfeng Chemicals Co. Ltd., China. The polymerizable surfactant, sodium 3-methacryloyloxy-2-hydroxy propane sulphonate (trade name: HPMAS), was supplied by Guangzhou Shuangjian Trading Co. Ltd., China. The radical initiator, benzoyl benzenecarboxperoxy (trade name: BPO), was supplied by Guangzhou Chemical Agent Factory, China. Acrylic acid and *N,N*-dimethylbenzylamine (DMBA) were purchased from Guangzhou Chemical Regents Co., China. Four photoinitiators were used: 2-isobutoxy-2-phenyl-acetophenone (trade name: benzoin butyl ether) supplied by Guangdong Hui Lian Da Chemical Industry Co. Ltd., China; 2-benzyl-2-dimethylamino-1-(4-morpholin-4-ylphenyl)butan-1-one (trade name: Irgacure 369), 2,2-dimethoxy-1,2-diphenyl-ethanone (trade name: Irgacure 651) and 2-methyl-1-(4-methylthiophenyl)-2-morpholinopropan-1-one (trade name: Irgacure 907) by Huntsman Co., China. The crosslinking agent, pentaerythritol triacrylates (PETA), was provided by Tianjin Tian Jiao Chemical Industry Co. Ltd., China. All the materials were used as received without further purification. Fig. 1 shows

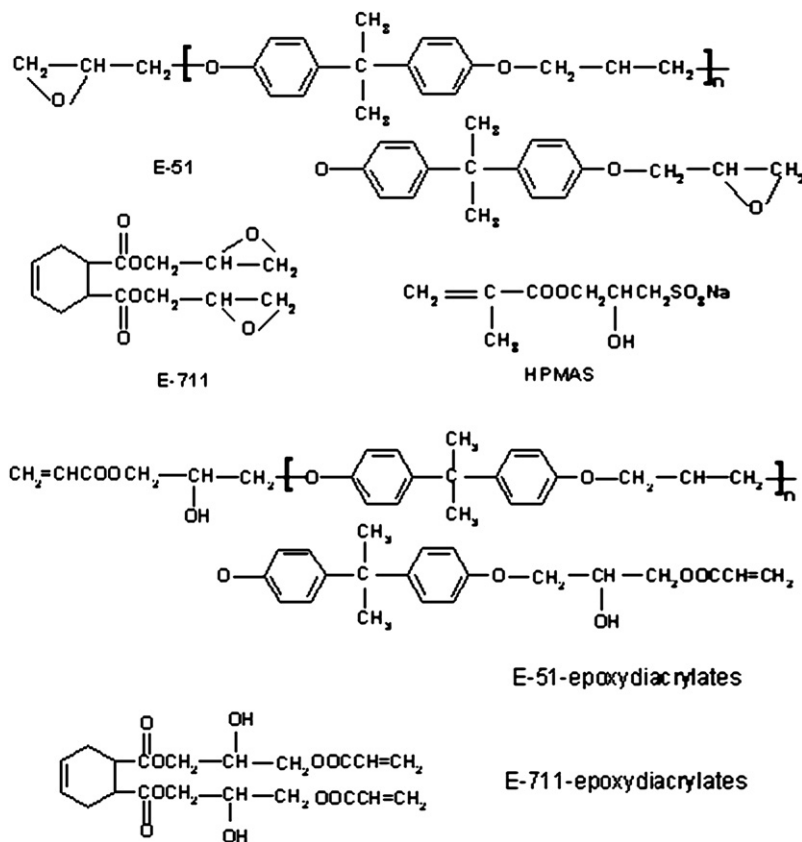


Fig. 1. Molecular structures of epoxy resins (E-51 and E-711), polymerizable emulsifier HPMAS, and epoxydiacrylates (E-51-epoxydiacrylates and E-711-epoxydiacrylates).

chemical structures of the aforementioned epoxy resins, epoxydiacrylates (to be synthesized as described below), and polymerizable emulsifier.

## 2.2. Preparation of epoxydiacrylates

Epoxydiacrylates, the photosensitive oligomers, were prepared from the reaction between the epoxy resin (E-51 or E-711) and acrylic acid. The reaction proceeded at 110 °C for 7 h in the presence of 0.05% (w/w) catalyst DMBA until the acid number reached a value of 4 mg KOH/g. For the convenience of discussion, the resultants were denoted as E-51-epoxydiacrylates or E-711-epoxydiacrylates, respectively. The acid number was determined by the following procedure. The sample (0.5–1 g) was filled into a conical flask with 40 ml ethanol and 1 ml phenolphthalein color indicator. The mixture was titrated by 0.1 mol/l KOH solution until pink color lasted for 30 s. The acid number was calculated by:

$$\text{Acid number, } D = \frac{N \times V \times 56}{G} \quad (1)$$

where  $N$  denotes the concentration of KOH solution,  $V$  is the volume of the consumed KOH solution, and  $G$  is the sample weight.

## 2.3. Preparation of SMANa emulsifier

Styrene (32.5 g, 0.306 mol), BPO (0.31 g) and 300 ml toluene were charged into a 1000 ml round bottom flask fitted with a nitrogen bubbler, magnetic stir bar, and condenser. After bubbling with nitrogen for 30 min, the reaction mixture was heated to 80 °C, and maleic anhydride (30 g, 0.306 mol) and BPO (0.31 g) dissolved in 300 ml toluene were added dropwise over 1 h. The reaction proceeded for an additional 4 h under stirring. Eventually, the alternating styrene–maleic anhydride copolymer (SMA) was filtered, washed with toluene and methanol, and dried at 80 °C under reduced pressure for 48 h. Details of the above procedures can be found in Ref. [12]. The resultant's number-average molecular weight ( $M_n = 11\,000$ ) and its distribution ( $M_w/M_n = 2.5$ ) were determined by gel permeation chromatography (GPC, Walter 208LC gel permeation chromatograph). The produced SMA (5 g) was saponified in 100 g NaOH aqueous solution (10%) for 5 h at 80 °C with stirring, and then the extra NaOH was neutralized by acid to give a light yellow solution of SMANa.

## 2.4. Preparation of epoxy-containing microcapsules

SMANa (3 g) solution was mixed with 100 g deionized water in a 200 ml beaker; and then, the mixture of 8.5 g epoxy resin (E-51 or E-711), 1.5 g epoxydiacrylates, 3.0 g HPMAS, including 0.5% PETA and 1.0% benzoin butyl ether, was added dropwise under vigorous stirring over 1 min to the aqueous phase to form an oil-in-water emulsion. After that the resultant emulsion was stirred with a homogenizer at 12 000 rpm for an additional 5 min. By using the apparatus shown in

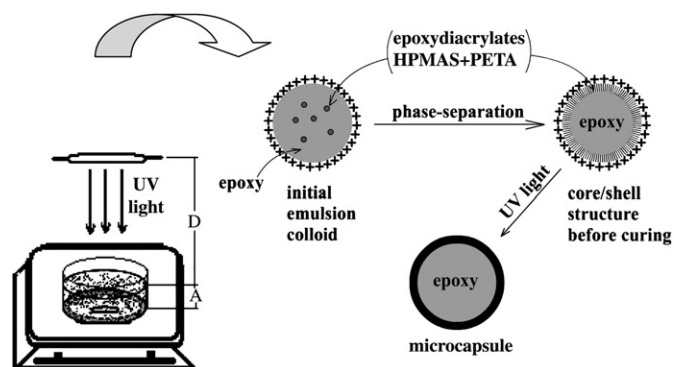


Fig. 2. The device for preparing the microcapsules and the proposed mechanism of solvent-induced phase separation.

Fig. 2, the emulsion was irradiated by UV light (3 kW high-pressure mercury lamp) for 3–15 min at room temperature. By precipitating the irradiated emulsion into a fivefold excess of water, the microcapsules were isolated, and then collected in a centrifuge tube, and washed with water several times. At last, the powder-like microcapsules were generated after drying in a vacuum freeze dryer.

To optimize the effect of UV irradiation conditions on the yield of microcapsules, an orthographic factorial design of five factors (i.e. depth of emulsion, irradiation time, UV lamp power, distance between UV lamp and the upper surface of the emulsion, and initiator concentration) and four-level was used (Table 1). The microcapsule yield was calculated by:

$$\text{Yield of microcapsules} = W_c/W_0 \times 100\% \quad (2)$$

where  $W_0$  represents the theoretical weight of the resultant microcapsules, i.e. the input weight of epoxy and wall-formers,  $W_c$  the weight of the obtained microcapsules after removing the unreacted wall-formers, homopolymer and unencapsulated epoxy. It is presumed that the wall materials are sufficient to encapsulate all the epoxy resin. Thus, the weight of the epoxy-containing microcapsules is proportional to their wall weight; the latter was determined by extracting the ground microcapsules with acetone for 48 h.

A control experiment was done as follows, using the same emulsion but a thermal initiator. Emulsion (100 ml) was

Table 1  
Creation of an orthographic factorial design of five factors and four levels for microcapsules preparation under UV irradiation

Level	Factor	Emulsion depth <sup>a</sup> , A (cm)	Irradiation time, t (min)	Lamp power, P (W)	Distance <sup>b</sup> , D (cm)	Initiator concentration <sup>c</sup> , C (%)
1	1	15	3000	10	2.0	
2	3	10	2500	15	1.5	
3	5	5	2000	20	1.0	
4	7	3	1500	25	0.5	

<sup>a</sup> Emulsion depth: distance from the top to the bottom of the emulsion (see Fig. 2).

<sup>b</sup> Distance: distance between UV lamp and the upper surface of the emulsion (see Fig. 2).

<sup>c</sup> Initiator: benzoin butyl ether.

charged into a three-neck flask (~250 cc) fitted with a nitrogen bubbler, magnetic stir bar and condenser. Under protection of nitrogen and stirring at 500 rpm, 10 ml initiator (0.6% ammonium persulfate solution) was added dropwise to the emulsion. The reaction proceeded for 3–7 h at 70 °C. The product was poured into large amount of water to remove the emulsifier. The microcapsules were collected in a centrifuge, and washed with water for several times. Finally, the powder-like microcapsules were obtained after drying in a vacuum freeze dryer.

## 2.5. Characterization

Morphology of the microcapsules was observed by an XL30 FEG scanning electron microscope (SEM), while their sizes were measured with a MasterSizer 2000 size analyzer. The composition of the microencapsulated epoxy (ground sample) was characterized by a Nexus 670 Fourier transform infrared spectroscope (FTIR). The thermal degradation behavior of the microcapsules was characterized by a Netzsch TG-209 thermogravimeter (TGA) in N<sub>2</sub> at a heating rate of 20 °C/min.

Reactivity of the epoxy core with the curing agent, 4,4'-diaminodiphenylsulfone (DDS), was detected by differential scanning calorimetry (DSC, 2910 MDSC, TA) at various heating rates under N<sub>2</sub>.

## 2.6. Determination of the microcapsules' core content

The core content of the resultant microcapsules was determined by extraction with acetone. Firstly, the microcapsule samples were ground with a mortar and pestle at room temperature. A certain amount of the dried and ground microcapsules ( $W_0$ ) was sealed in a filter paper bag. Then, the bag with the ground microcapsules was dried for 5 h in a vacuum oven at 55 °C, cooled in a vacuum desiccator and precisely weighed ( $W_1$ ). Afterwards, the sample bag was placed in a Soxhlet apparatus, extracted with acetone for 24 h, and dried in a vacuum oven at 55 °C. After cooling in a vacuum desiccator, the sample bag was weighed again ( $W_2$ ). Eventually, the core content of the microcapsules,  $\alpha$ , was calculated by:

$$\alpha = \frac{W_1 - W_2}{W_0} \times 100\% \quad (3)$$

## 3. Results and discussion

### 3.1. Characterization of the epoxy-containing microcapsules

Emulsification of the epoxy phase containing epoxydiacrylates and HPMAS as wall-formers in the continuous aqueous phase offers the possibility of forming capsules by virtue of interfacial polymerization induced by UV irradiation. During emulsification, each wall-former, especially HPMAS, tends to partition into the aqueous phase while minute amounts of water diffuse into the oil phase. The epoxydiacrylates and

HPMAS, which are not completely soluble in epoxy resin, tend to separate and congregate at the interface between the emulsion colloid and water. This process is ascribed to the desirable solvent-induced phase separation as shown in Fig. 2. That is, the hydrophilic wall-formers are driven to form colloidal shells.

The mechanism of the solvent-induced phase separation can be further understood by the interaction among the emulsifier, epoxydiacrylates and HPMAS. Meanwhile, HPMAS plays a dual role as emulsifier and polymerizable wall-former. As a water-soluble chemical, HPMAS definitely has an affinity for water and acts as an emulsifier at the colloid surface. On the other hand, since two hydroxyl groups will be formed during the reaction of epoxy with acrylic acid, epoxydiacrylates are more likely located at the outer layer of the emulsion colloid due to the interaction between hydroxyl and carbonyl groups attached to the emulsifiers, i.e. SMANa and HPMAS. As a result, whenever the emulsion is exposed to UV light, free radical copolymerization of epoxydiacrylates with HPMAS would be initiated to form the shell polymer. Even if the epoxydiacrylates cannot accumulate completely near the aqueous phase, the copolymer of epoxydiacrylates with HPMAS would be more hydrophilic than the epoxy resin. Eventually, the microcapsules with epoxy as core and the copolymer as shell are produced.

The capsule formation analyzed above can be proved by the following experimental results. Under UV irradiation, the shell phase containing the wall-formers was cured into a solid. As shown in Fig. 3(a), the resulting microcapsules have relatively uniform sizes. No destruction of the capsule walls due to mechanical agitation is perceivable. When the capsule has been artificially crushed, a core-shell structure rather than solid particle or porous structure can be identified (Fig. 3(c)). The wall thickness is estimated at ~300 nm according to Fig. 3(d) that shows a microcapsule of ~30  $\mu$ m in diameter. Besides, both the inner and the exterior surfaces of the microcapsule are quite smooth (Fig. 3(b) and (f)), but actually the shell is composed of many layers (Fig. 3(e)). These morphological features correlate well with the prediction of capsule formation made on the basis of solvent-induced phase separation.

FTIR spectra of the uncured epoxy (E-51), E-51-containing microcapsules, and the shells that were obtained by grinding the microcapsules and then acetone extraction are shown in Fig. 4. Evidently, the epoxide groups inside the microcapsules are detectable as characterized by their distinct peaks at 980, 910 and 771  $\text{cm}^{-1}$ . These results suggest that the structure of epoxy resin remains unchanged after encapsulation. On the other hand, for both the shells and the microcapsules, the characteristic absorption peaks of carbonyl and sulfonic groups were moderately visible at 1739 and 1175  $\text{cm}^{-1}$ , respectively, indicating that the shells are composed of epoxydiacrylates and HPMAS as expected.

The core content of the microcapsules can be measured by subtracting the shell weight from that of the capsules and lies in the range from 54 to 71% for the capsules of 5–35  $\mu$ m in diameter. The larger microcapsules contain larger amount of

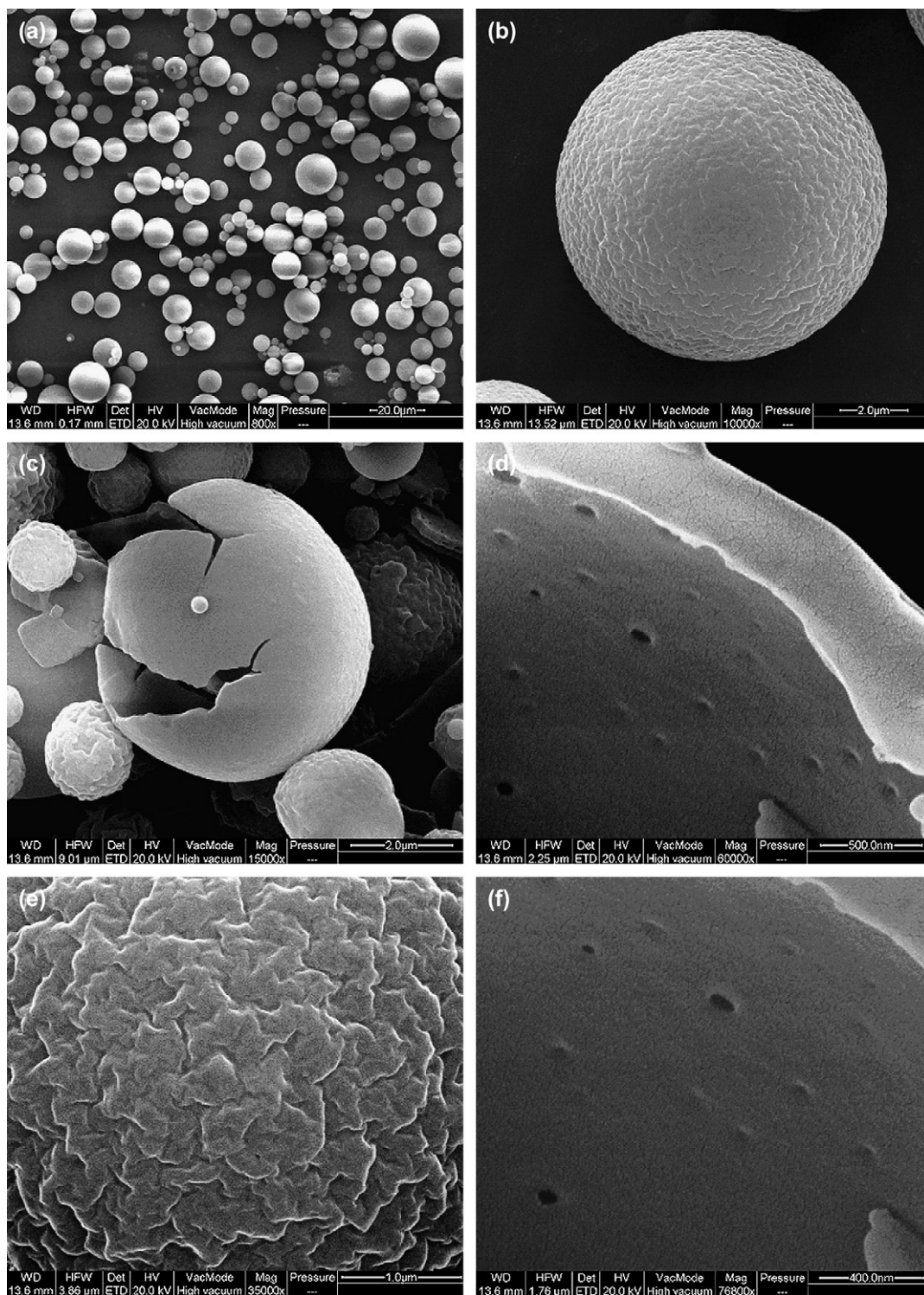


Fig. 3. SEM photos of E-711-containing microcapsules. (a and b) Appearance of the microcapsules, (c) crushed microcapsule, (d) close view of the capsule shell, (e) exterior surface of a microcapsule, and (f) interior surface of a microcapsule.

epoxy. This might result from the fact that the microcapsules' shells become thinner with the expansion of capsules. Therefore, the microcapsules with larger size should contain larger proportions of the core substance (i.e. epoxy).

The core–shell structure of the microcapsules is further revealed by their pyrolytic behavior. As illustrated in Fig. 5 and Table 2, both neat epoxy and shells show one stage of thermal

decomposition, while the latter starts to decompose at higher temperature owing to its crosslinked structure. Accordingly, the microcapsules exhibit two stages of weight loss with a rise in temperature. The first stage is attributed to the degradation of core epoxy, while the second one corresponds to the shell decomposition. Compared to neat epoxy (curves 1 and 2 in Fig. 5), thermal stability of the epoxy encapsulated in the

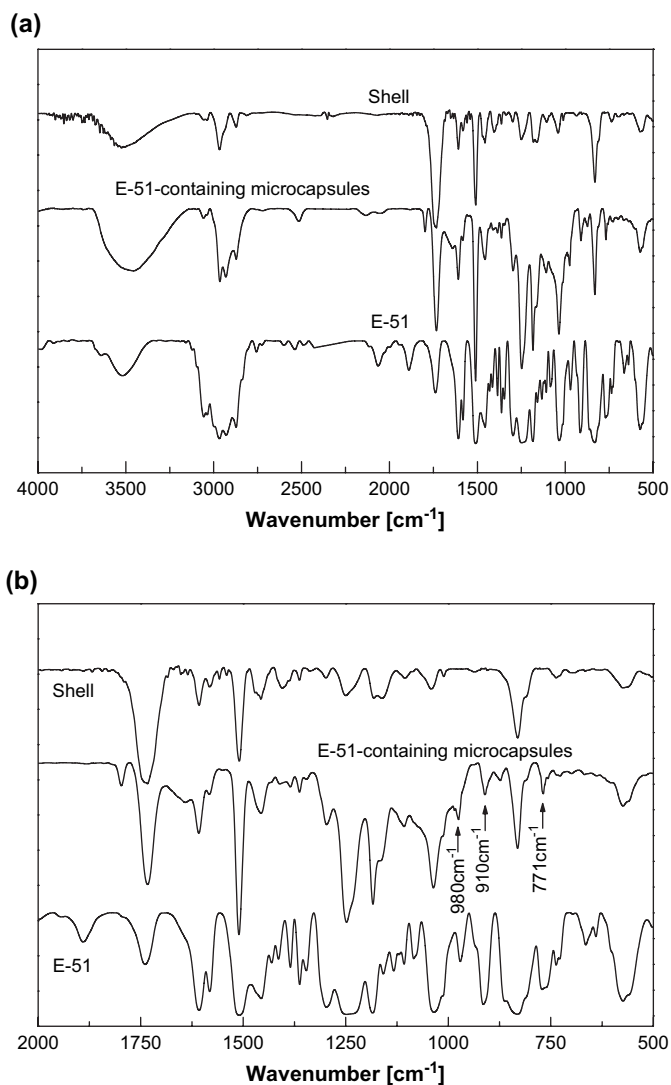


Fig. 4. FTIR spectra of E-51, E-51-containing microcapsules and the shells made from E-51-epoxydiacrylates/HPMAS. (a) The entire spectra and (b) amplified portion of the spectra from 500 to 2000  $\text{cm}^{-1}$ .

microcapsules (curves 3 and 4 in Fig. 5) is markedly increased owing to the protection of the shells. Meanwhile, decomposition of the shells of the microcapsules (refer to the second pyrolytic stages of curves 3 and 4 in Fig. 5) also occurs at higher temperature than neat shells (curve 5 in Fig. 5), implying that certain reaction might exist between the core and shell at high temperature. It manifests that the core and shell materials become more stable when they are combined into the microcapsules.

It is worth noting that E-51-containing microcapsules possess higher thermal stability than that of E-711-containing microcapsules. In this context, the former is more appropriate for manufacturing self-healing epoxy composites with high temperature curing agent. Besides, as the viscosity of E-51 epoxy is about 10–16 Pa s, while that of E-711 is only 0.45–0.6 Pa s, E-711-containing microcapsules would be beneficial to self-healing at or below room temperature.

The effect of epoxydiacrylates is illustrated in Fig. 6. Without epoxydiacrylates, the surface of the microcapsules made

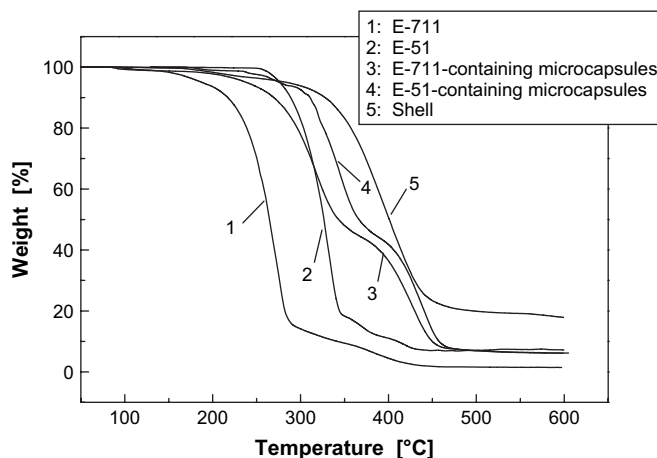


Fig. 5. TGA curves of unsealed epoxy, epoxy-containing microcapsules and the shells made from E-51-epoxydiacrylates/HPMAS.

from amine acrylate and HPMAS copolymer is rough and wizened (Fig. 6(a)). A few broken capsules are observed, indicating that they are somewhat fragile. In fact, the crimped surface reflects high shrinkage resulting from copolymerization between the low molecular weight amine acrylate and HPMAS. In contrast to the case shown in Fig. 6(a), the microcapsules based on epoxydiacrylates and HPMAS have much smoother surfaces (Fig. 6(b) and (c)). In addition, E-51-epoxydiacrylates perform better than E-711-epoxydiacrylates in constructing the microcapsule surface. This phenomenon may be due to the fact that E-51-epoxydiacrylates possess more hydroxyl groups than E-711-epoxydiacrylate and hence, acquire higher hydrophilicity in favor of building uniform shell layers.

With respect to the crosslinking agent, PETA, its role in improving thermal stability of the microcapsules can be seen in Fig. 7. Although epoxydiacrylate might also act as a crosslinking agent owing to the two double bonds at its molecular ends, introduction of PETA that possesses three double bonds would undoubtedly increase the crosslinking density of the shells.

Since the epoxy-containing microcapsules are prepared for producing self-healing epoxy composites, reactivity of the

Table 2  
Pyrolytic characteristics of epoxy, epoxy-containing microcapsules and capsule shells made from E-51-epoxydiacrylates/HPMAS

Material	First pyrolytic stage			Second pyrolytic stage		
	$T_{1, \text{onset}}^a$ (°C)	$T_{1, \text{p}}^b$ (°C)	$T_{1, \text{end}}^c$ (°C)	$T_{2, \text{onset}}^a$ (°C)	$T_{2, \text{p}}^b$ (°C)	$T_{2, \text{end}}^c$ (°C)
E-51	306	327	342	—	—	—
E-711	242	276	288	—	—	—
E-51-containing microcapsules	314	339	358	420	436	450
E-711-containing microcapsules	268	294	328	399	421	449
Shells	—	—	—	362	398	418

<sup>a</sup>  $T_{1, \text{onset}}$ ,  $T_{2, \text{onset}}$ : onset temperatures of the first and second pyrolytic stages, respectively.

<sup>b</sup>  $T_{1, \text{p}}$ ,  $T_{2, \text{p}}$ : peak temperatures of the first and second pyrolytic stages, respectively.

<sup>c</sup>  $T_{1, \text{end}}$ ,  $T_{2, \text{end}}$ : end temperatures of the first and second pyrolytic stages, respectively.

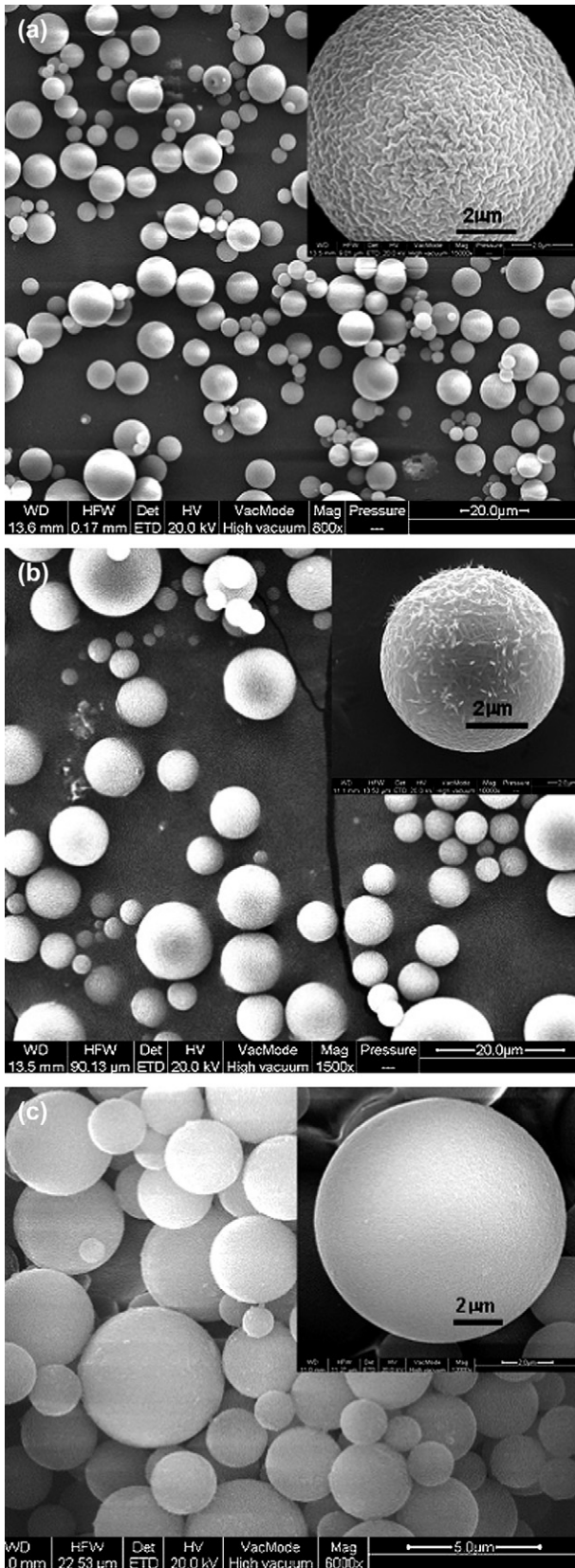


Fig. 6. SEM photos of E-711-containing microcapsules. The shells were made from: (a) amine acrylate/HPMAS, (b) E-711-epoxydiacrylates/HPMAS, and (c) E-51-epoxydiacrylates/HPMAS.

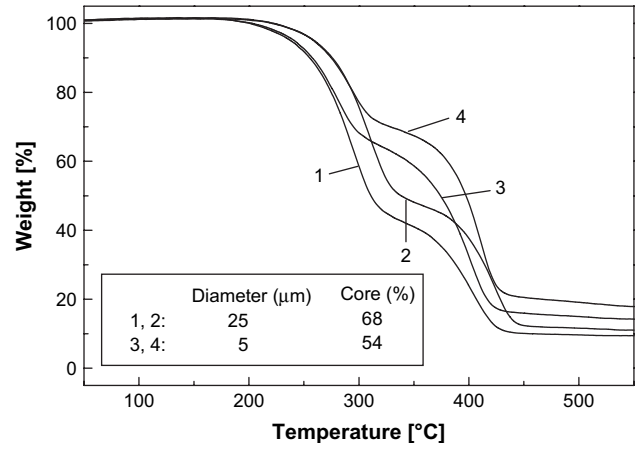


Fig. 7. TGA curves of E-711-containing microcapsules (1 and 3) without curing agent PETA; (2 and 4) with curing agent PETA.

encapsulated epoxy should be explored. Accordingly, a model mixture consisting of stoichiometric encapsulated epoxy (that was obtained by grinding the microcapsules) with curing agent DDS was heated and monitored by DSC at different heating

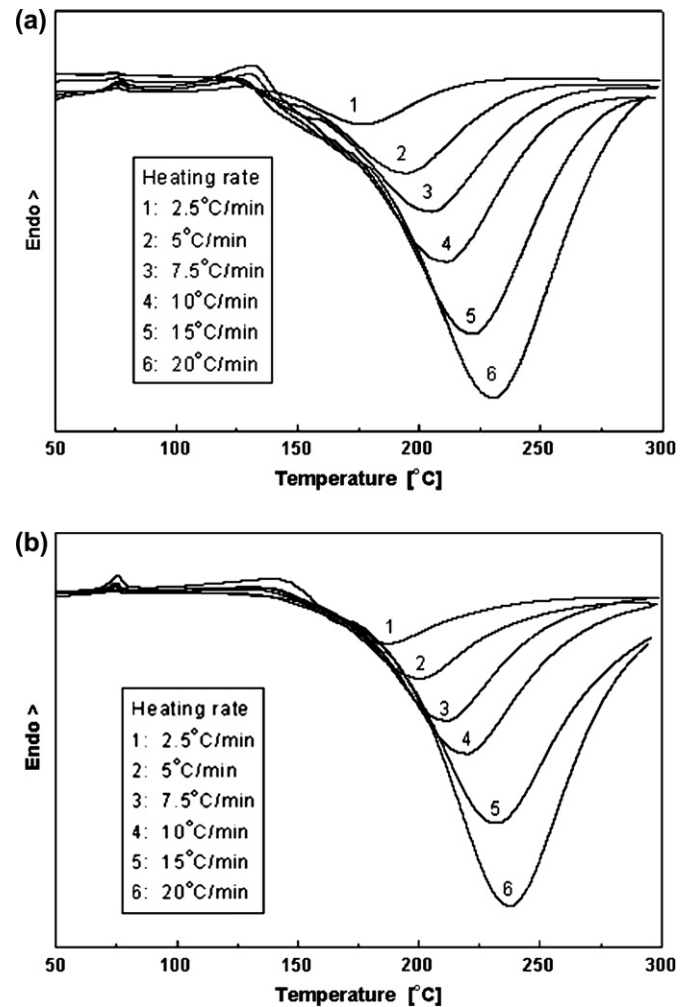


Fig. 8. DSC heating traces of (a) encapsulated epoxy (obtained from the ground E-51-containing microcapsules)/DDS (100/30) and (b) E-51/DDS 100/32 systems.

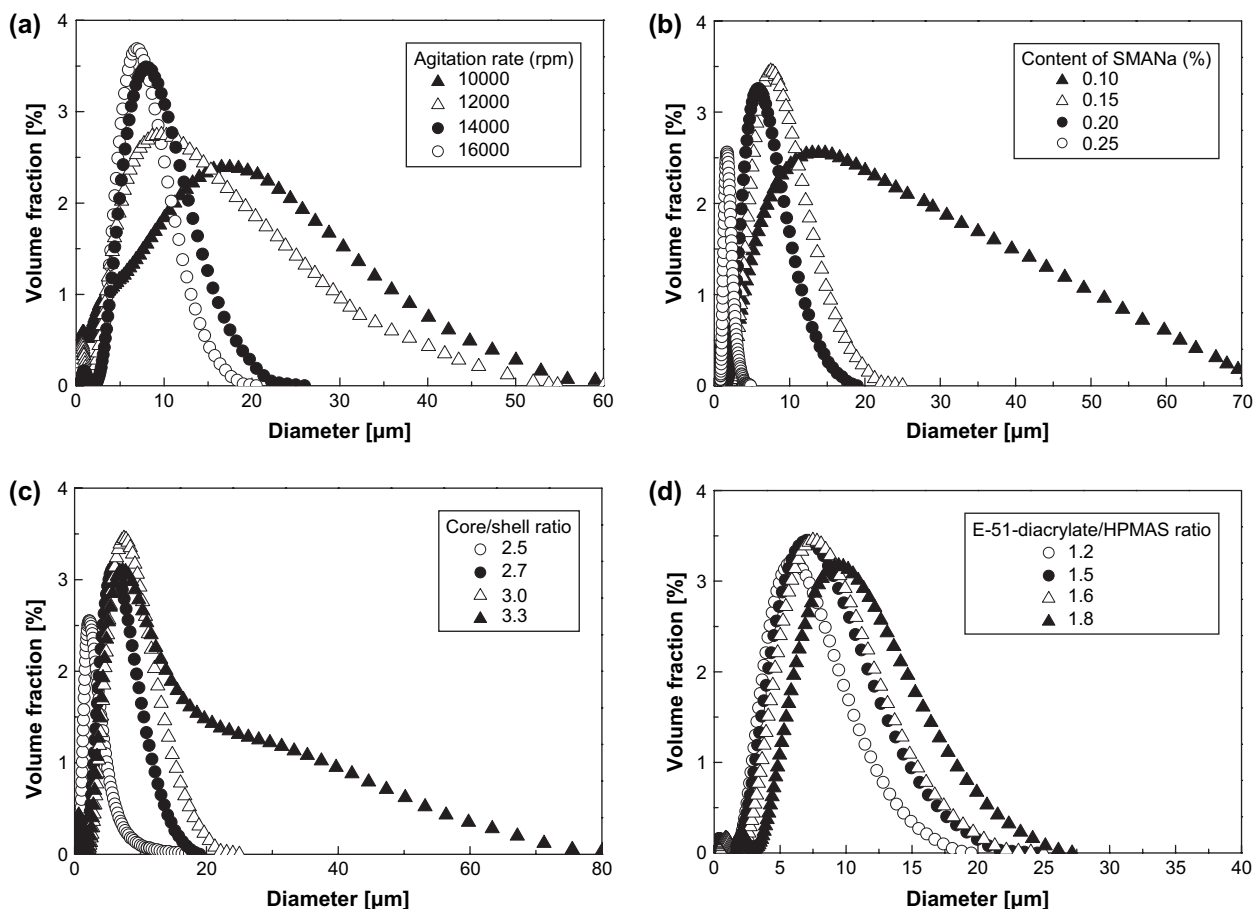


Fig. 9. Size distribution of E-711-containing microcapsules. Preparation conditions: (a) core/shell ratio = 3.0, E-51-epoxydiacrylates/HPMAS ratio = 1.6, SMANa content = 0.15%; (b) core/shell ratio = 3.0, E-51-epoxydiacrylates/HPMAS ratio = 1.6, agitation rate = 14 000 rpm; (c) E-51-epoxydiacrylates/HPMAS ratio = 1.6, SMANa content = 0.15%, agitation rate = 14 000 rpm; (d) core/shell ratio = 3.0, SMANa content = 0.15%, agitation rate = 14 000 rpm.

rates (Fig. 8(a)). It is seen that the exothermic peaks of encapsulated epoxy/DDS are similar to the control epoxy/DDS system (Fig. 8(b)). By using the well-known Kissinger equation [16], the activation energy of the reaction of encapsulated epoxy/DDS pair was estimated to be 66.9 kJ/mol, which is almost the same as the value of epoxy/DDS system (66.0 kJ/mol), which means that the epoxy resin inside the microcapsules retains its reactivity.

### 3.2. Influencing factors of preparation of the epoxy-containing microcapsules

As discussed above, the epoxy-containing microcapsules are produced via emulsification of epoxy resin followed by UV-induced in situ polymerization of the wall-formers. Therefore, all the factors that determine size and size distribution of colloid particles should affect the size of the microcapsules. In this section, the variation in microcapsules' size is investigated by changing agitation rate, content of SMANa, core/shell weight ratio, and epoxydiacrylates/HPMAS weight ratio.

Fig. 9(a) shows the influence of agitation rate during emulsification on size distribution of the microcapsules. Clearly, increasing the agitation rate reduces the microcapsules' size and narrows the size distribution. This effect is less significant

when the agitation rate exceeds 14 000 rpm. The SEM observation in Fig. 10 further gives a direct view of the phenomenon that a higher agitation rate leads to smaller microcapsules. Nevertheless, the surface appearance of the microcapsules of different sizes is similar. These results are likely the reflection of the fact that the colloid size decreases along with increasing agitation rate. Fig. 9(b) shows that the size and size distribution of the microcapsules decrease with increasing emulsifier dosage. This proves that the microcapsules' size is indeed correlated with the emulsion colloid size.

In addition, the microcapsules' size is proportional to the core content. Raising the core/shell ratio would enlarge the capsules and broaden their size distribution (Fig. 9(c)). This phenomenon is consistent with the general law of capsule preparation. In the experiments conducted in this work, the core/shell ratios are sufficient for constructing microcapsules with core/shell structure. In case of an extremely low core/shell ratio, however, porous particles might be prepared. When the core/shell ratio is too high, on the contrary, a certain amount of the core substance might not be encapsulated. The upper and lower limits of the core/shell ratio should be studied further.

Dependence of the microcapsules' size on epoxydiacrylates/HPMAS ratio is shown in Fig. 9(d). With a rise in



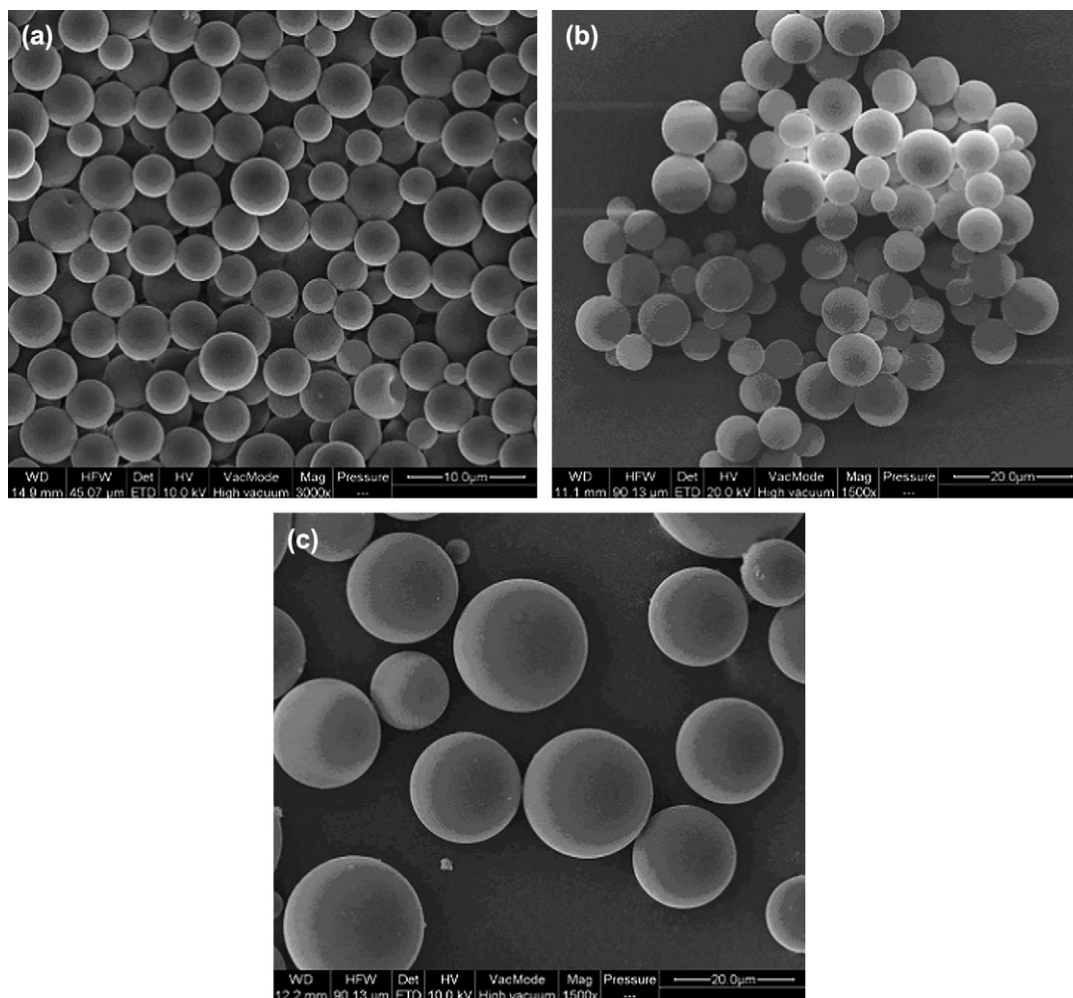


Fig. 10. SEM photos of E-711-containing microcapsules prepared at different agitation rates: (a) 18 000 rpm (average size = 3.2  $\mu\text{m}$ ); (b) 14 000 rpm (average size = 10.5  $\mu\text{m}$ ); (c) 12 000 rpm (average size = 18.7  $\mu\text{m}$ ). SMANa content in all the systems was set at 0.15%.

epoxydiacrylates/HPMAS ratio, size and size distribution of the microcapsules both moderately increase. This should be related to the functions of the two chemicals. Epoxydiacrylate is an oligomer, while HPMAS plays dual roles as monomer and emulsifier. Less HPMAS might reduce emulsion stability, leading to larger capsules and wider size distribution of the capsules.

The present work deals with the preparation of epoxy-containing microcapsules using UV irradiation. Undoubtedly, influence of the conditions of UV irradiation should be carefully studied. For this purpose, orthographic factorial design was applied and the microcapsule yield was set as the response of the designed experiments. Table 3 and Fig. 11 show the results and analysis of the effects of the five factors at four levels (refer to Table 1).

From Fig. 11, it is found that emulsion depth has a very evident influence on the capsule yield. The emulsion can absorb and reflect UV light. Accordingly, in the depths of the emulsion the light intensity has to be weakened so that the yield is reduced. Similarly, lower yields are attained by reducing irradiation time, or lowering the lamp power, or increasing the distance between the lamp and the emulsion, as a result of

decreasing UV light intensity. In general, the differences in the yield at different levels are moderate except for the emulsion depth. In particular, the initiator concentration has nearly no influence on the capsule yield within the range of interests.

The data in Fig. 11 indicate that the experiments carried out at level 1 give the highest capsule yield. However, it does not mean that the optimum conditions can thus be concluded because of the complicated situation in practice. For example, the emulsion depth is the most important factor for the capsule yield and the thinner emulsion depth results in higher yield, but the emulsion with too thin depth (1 cm) does not favor its stirring. As a result, 3 cm depth of the emulsion filled in a reverse conical beaker is suggested. For irradiation time and lamp power, since levels 1 and 2 show similar results, level 2 is chosen for energy saving. The distance between the UV lamp and the emulsion is selected at level 1, while the initiator concentration is fixed at level 4 for cost control. In summary, the optimum conditions for the UV irradiation-aided encapsulation are: 3 cm for emulsion depth, 10 min for irradiation time, 2.5 kW for lamp power, 10 cm for the distance between the UV lamp and the emulsion, and 0.5% for the photoinitiator.

Table 3  
Result analysis of the orthographic factorial design for microcapsules' preparation under UV irradiation

Level	Factor <sup>a</sup>						Microcapsule yield (%)
	A	t	P	D	C		
	1	2	3	2	3	80.2	
	3	4	1	2	2	60.4	
	2	4	3	3	4	66.3	
	4	2	1	3	1	63.1	
	1	3	1	4	4	76.5	
	3	1	3	4	1	61.8	
	2	1	1	1	3	81.5	
	4	3	3	1	2	58.4	
	1	1	4	3	2	79.9	
	3	3	2	3	3	63.3	
	2	3	4	2	1	68.9	
	4	1	2	2	4	64.8	
	1	4	2	1	1	76.4	
	3	2	4	1	4	66.5	
	2	2	2	4	2	74.8	
	4	4	4	4	3	50.9	
Result analysis							
$K_{1j}^b$ (%)	313.0	288.0	281.6	282.8	270.2	—	
$K_{2j}$ (%)	291.6	284.7	279.2	274.2	273.4	—	
$K_{3j}$ (%)	251.9	267.1	266.8	272.6	275.9	—	
$K_{4j}$ (%)	237.1	253.9	266.1	264.1	274.2	—	
$Y_{1j}^c$ (%)	78.3	72.0	70.4	70.7	67.6	—	
$Y_{2j}$ (%)	72.9	71.2	69.8	68.6	68.4	—	
$Y_{3j}$ (%)	63.0	66.8	66.7	68.1	69.0	—	
$Y_{4j}$ (%)	59.3	63.5	66.5	66.0	68.5	—	

<sup>a</sup> The symbols denoting the five factors have the same meaning as those in Table 1.

<sup>b</sup>  $K_{ij}$  denotes the sum of microcapsule yield with level  $i$  and factor  $j$ .

<sup>c</sup>  $Y_{ij}$  denotes the average of  $K_{ij}$ .  $Y_{ij} = K_{ij}/N_j$ ,  $N_j$  is the number of level  $i$  with the same factor  $j$ .

### 3.3. Formation kinetics of the microcapsules

To reveal formation kinetics of the microcapsules, dependencies of capsule yield on UV irradiation time are shown in Fig. 12. For all the systems, regardless of the photoinitiator species, the reaction rates are rather high within the first few minutes and then level off. Compared to the systems initiated by benzoin butyl ether, Irgacure 651 and Irgacure 907 that have similar equilibrium capsule yields of about 80%, the

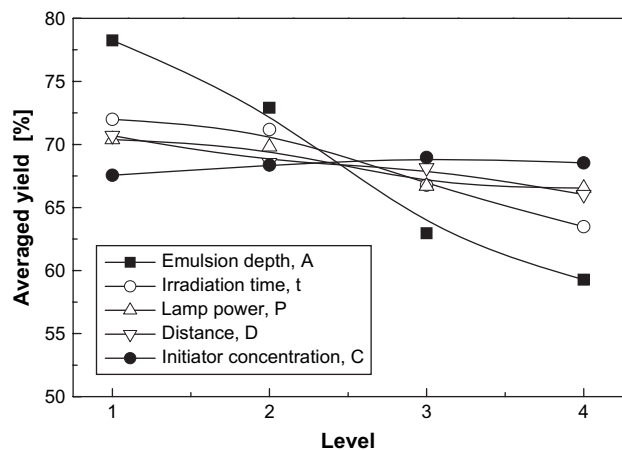


Fig. 11. Influence of different levels of the five factors (see Table 1) on the averaged capsule yield (that was taken from the values of  $Y_{ij}$  listed in Table 3).

system with Irgacure 369 presents a significantly lower yield. The results might be related to the structures of the radicals originating from photodecomposition (Fig. 13). One of the radicals coming from Irgacure 369 has a phenyl group, which should set up a higher steric hindrance to the access of monomers.

A careful survey of Fig. 12 indicates that there is no induction period at the early stage of polymerization for the systems

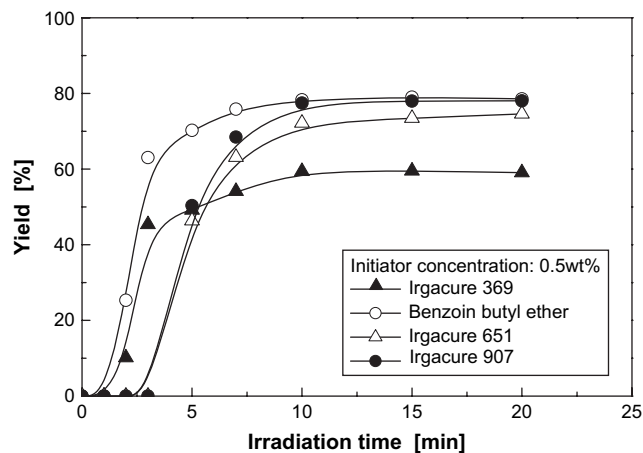


Fig. 12. UV irradiation time dependence of microcapsule yield initiated by different photoinitiators. Irradiation conditions: emulsion depth = 3 cm, irradiation time = 10 min, lamp power = 2.5 kW, distance between UV lamp and the emulsion = 10 cm, initiator concentration = 0.5%.

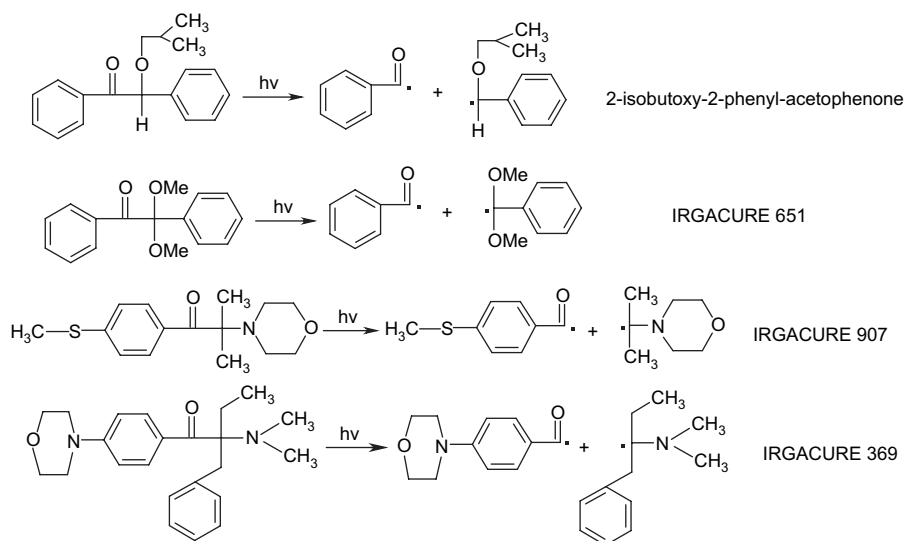


Fig. 13. Photodecomposition of the initiators.

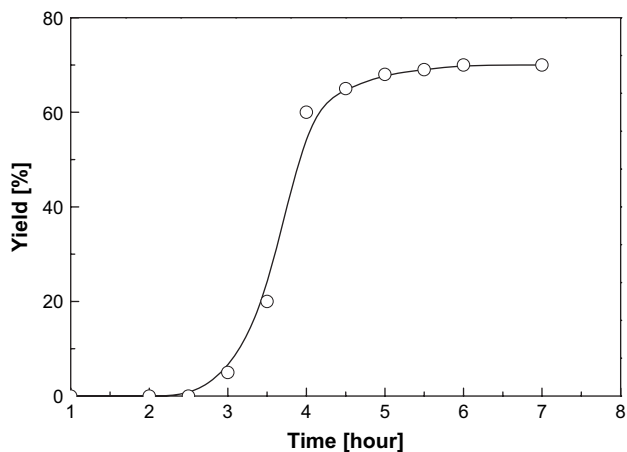


Fig. 14. Dependence of microcapsule yield on reaction time of the system with the thermal initiator. Reaction conditions: core/shell ratio = 3.0, E-51-epoxydiacrylate/HPMAS rate = 1.6, SMANa content = 0.15%, agitation rate = 14 000 rpm.

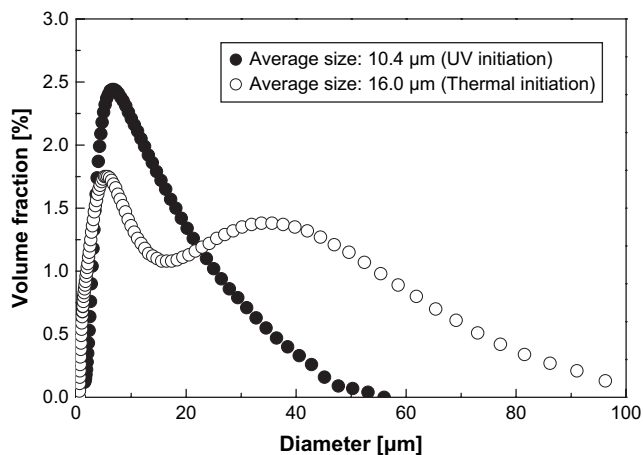


Fig. 15. Size distributions of E-711-containing microcapsules prepared by different methods.

with benzoin butyl ether and Irgacure 369, while an induction period of 3 min is required for the systems with Irgacure 651 and Irgacure 907. In the former cases, under the irradiation of UV light, a great deal of free radicals are produced in a short time and start to initiate copolymerization of epoxydiacrylates with HPMAS immediately. As a result, the inhibitor resolved in the system becomes negligible and has no retardation effect. The induction period observed in conventional free radical polymerization is instead replaced by a high-speed conversion period. In contrast, for the latter cases, the amount of free radicals is not enough to quickly consume the inhibitor so that the induction period appears. Whereas, it seems that the ultimate capsule yield has nothing to do with the induction period.

To highlight the advantage of the emulsion encapsulation induced by UV light, a control experiment was done using the same emulsion except that a water-soluble initiator  $(\text{NH}_4)_2\text{S}_2\text{O}_8$  was added instead of photoinitiators. As shown in Fig. 14, the microcapsules emerge after 3 h of the reaction, and 5 h are needed for completion of the reaction. In comparison with the encapsulation process induced by UV irradiation that is completed within 10 min, the thermally initiated encapsulation takes a much longer time. Besides, the microcapsules produced via thermal initiation have larger size and wider size distribution (Fig. 15). It may also be a result of the prolonged reaction. The emulsion colloids have enough time to collide with each other and to merge before curing of the shell layer. For the UV-induced reaction, the colloids can be solidified within a few minutes, leaving no time for changing the colloid size.

#### 4. Conclusions

A novel technique for producing epoxy resin-containing microcapsules was proposed on the basis of UV-induced interfacial polymerization in epoxy emulsion. Epoxydiacrylates and a polymerizable emulsifier were chosen as the

wall-formers. During the emulsification process, solvent-induced phase separation occurred within epoxy emulsion colloids, and then the exterior layer of the colloids accumulated by the wall-formers was copolymerized under UV irradiation to construct capsules' shells.

The resultant microcapsules have relatively uniform size (5–35  $\mu\text{m}$ ), smooth surface and thin wall thickness (200–300 nm). The core content lies in the range from 54 to 71%. The encapsulated epoxy retains its chemical feature and reactivity with curing agent as well. Due to protection of the shells, the epoxy sealed in the microcapsules exhibits higher thermal stability than its original version. These facilitate the future application of the microcapsules in making self-healing epoxy composites.

The microcapsules' size is closely related to that of epoxy colloids. Smaller capsules with narrow size distribution can be obtained by high-speed agitation or a high dosage of emulsifier. By analyzing the results of orthographic factorial design with respect to the effects of UV irradiation conditions on capsule yield, emulsion depth was found to be the most important influencing factor, while photoinitiator concentration had nearly no influence within the experimental range. As compared with thermally initiated system, the current approach aided by UV irradiation is much faster in terms of the time needed for preparing epoxy-containing microcapsules.

In addition to the chemicals employed in this work, many other photosensitive monomers and polymerizable emulsifiers are available for the newly proposed approach. Accordingly, structure and properties of the microcapsules' shells can be easily tailored to fulfill the requirements of practical application.

## Acknowledgements

The authors are grateful to the support of the Natural Science Foundation of China (Grants: 50573093, U0634001).

## References

- [1] Sawada K, Urakawa H. Preparation of photosensitive color-producing microcapsules utilizing in situ polymerization method. *Dyes Pigments* 2005;65:45–9.
- [2] Bohlmann JT, Schneider C, Andresen H, Buchholz R. Optimized production of sodium cellulose sulfate (NaCS) for microencapsulation of cell cultures. *Chem Eng Technol* 2002;2(12):384–8.
- [3] Matsunami Y, Ichikawa K. Characterization of the structures of poly(urea-urethane) microcapsules. *Int J Pharm* 2002;242:147–53.
- [4] Shulkin A, Stöver HDH. Polymer microcapsules by interfacial polyaddition between styrene–maleic anhydride copolymers and amines. *J Membr Sci* 2002;209:421–32.
- [5] White SR, Sottos NR, Geubelle PH, Moore JS, Kessler MR, Sriram SR, et al. Autonomic healing of polymer composites. *Nature* 2001;409:794–7.
- [6] Yuan L, Liang GZ, Xie JQ, Li L, Guo J. Preparation and characterization of poly(urea-formaldehyde) microcapsules filled with epoxy resins. *Polymer* 2006;47:5338–49.
- [7] Yin T, Rong MZ, Zhang MQ, Yang GC. Self-healing epoxy composites – preparation and effect of the healant consisting of microencapsulated epoxy and latent curing agent. *Compos Sci Technol* 2007;67:201–12.
- [8] Yuan L, Liang GZ, Xie JQ, Guo J, Li L. Thermal stability of microencapsulated epoxy resins with poly(urea-formaldehyde). *Polym Degrad Stab* 2006;91:2300–6.
- [9] Matson GW. Microcapsules and process of making. U.S. Patent 3,516,941; 1970.
- [10] Foris PL, Brown RW, Phillips PS. Capsule manufacture. U.S. Patent 4,100,103; 1978.
- [11] Deasy PB. Microencapsulation and related drug processes. New York: Marcel Dekker; 1984. p. 119, 219.
- [12] Chang TMS. Artificial cells with emphasis on bioencapsulation in biotechnology. *Biotechnol Annu Rev* 1995;1:267–95.
- [13] Quek CH, Li J, Sun T, Chan MLH, Mao H-Q, Gan LM, et al. Photocrosslinkable microcapsules formed by polyelectrolyte copolymer and modified collagen for rat hepatocyte encapsulation. *Biomaterials* 2004;25:3531–40.
- [14] Shen F, Li AA, Cornelius RM, Cirone P, Childs RF, Brash JL, et al. Biological properties of photocrosslinked alginate microcapsules. *J Biomed Mater Res Appl Biomater* 2005;75B:425–34.
- [15] Chattopadhyay DK, Panda SS, Raju KVS. Thermal and mechanical properties of epoxy acrylate/methacrylates UV cured coatings. *Prog Org Coat* 2005;54:10–9.
- [16] Kissinger HE. Reaction kinetics in differential thermal analysis. *Anal Chem* 1957;29:1702–6.